Calculation of Position-Dependent Inductances of a Permanent Magnet Synchronous Machine With an External Rotor by Using Voltage-Driven Finite Element Analyses

Erich Schmidt and Andreas Eilenberger

Institute of Electrical Drives and Machines, Vienna University of Technology, Vienna 1040, Austria

This paper discusses finite element analyses of a skewed permanent magnet synchronous machine (PMSM) with an external rotor regarding the magnetic saliency. Since the machine is fed from a voltage source inverter (VSI), a simulation as close as possible to the regular operational behavior is intended. Therefore, a voltage-driven finite element model with a strong circuit coupling excited with the time-dependent voltages according to the space vectors of the VSI will be applied. This approach directly allows for a comparison of the numerically obtained phase currents with those obtained from measurements. Afterwards, the inductance characteristics depending on the rotor position can be evaluated from the time-dependent phase currents in order to obtain the suitability for a sensorless control algorithm.

Index Terms—**Finite element analysis, inform method, permanent magnet synchronous machine (PMSM), sensorless control.**

I. Introduction

TODAY, the permanent magnet synchronous machine (PMSM) with an external rotor gains more and more in importance. In particular, this comes from the automotive industry turnover to highly efficient PMSM utilized for hybrid drive solutions. For such an application, the torque ripple shows high significance and should be as small as possible.

One option for a small torque ripple is achieved by using skewed stator slots. In general, such an arrangement requires a 3-D finite element model and consequently long calculation times will arrive especially with voltage driven analyses. These drawbacks can be avoided by using separated 2-D models of rotor and stator, which are coupled only by floating boundary conditions in dependence on skewing and angular rotor position [1]–[4]. On the other hand, voltage driven analyses simulating the regular operational behavior of a voltage source inverter (VSI) can be carried out when using a strong coupling of finite element model and external circuit elements [5]. Thus, short calculation times for the position-dependent inductances of the PMSM are achieved.

The paper discusses voltage-driven finite element analyses of a PMSM with an external rotor for a comparison of the numerically obtained stator current waveforms and position-dependent inductances with the data obtained from measurements.

II. Space Vector Calculus

In the subsequent analyses for determining the operational behavior of the given machine, steady-state operation in conjunction with constant rotor angular velocity is supposed. All data are given in normalized values [6].

Manuscript received October 07, 2008. Current version published February 19, 2009. Corresponding author: E. Schmidt (e-mail: erich.schmidt@tuwien.ac.at)

Color versions of one or more of the figures in this paper are available online at http://ieeexplore.ieee.org.

Digital Object Identifier 10.1109/TMAG.2009.2012822

In the dq rotor fixed reference frame, the stator current and stator flux space vectors can be written as

$$\underline{i}_{S,dq} = i_S e^{\jmath\beta} = i_{S,d} + \jmath i_{S,q} \tag{1}$$

$$\underline{\psi}_{S,dq} = \psi_S e^{\jmath\vartheta} = \psi_{S,d} + \jmath\psi_{S,q} \tag{2}$$

where β, ϑ are the stator current angle and the stator flux angle, respectively. The components of the stator flux linkage are defined by

$$\psi_{S,d} = l_d i_{S,d} + \psi_M \tag{3a}$$

$$\psi_{S,q} = l_q i_{S,q} \tag{3b}$$

where l_d, l_q are the direct and quadrature axis inductances and ψ_M denotes the flux linkage of the permanent magnets.

In order to inject the stator currents in the finite element model, the stator current and stator flux space vectors are transformed as given by

$$\underline{i}_{S,\alpha\beta} = \underline{i}_{S,dq} e^{\jmath\gamma} \tag{4}$$

$$\underline{\psi}_{S,\alpha\beta} = \underline{\psi}_{S,dq} e^{\jmath\gamma} \tag{5}$$

where γ denotes the angular rotor position. As the stator winding is Y-connected, any zero sequence stator currents are impossible.

A. Complex Inform Reluctance

In case of $\psi_M = 0$ and neglecting the stator resistance, the constant rotor angular velocity allows for the definition of a complex stator admittance, which can be derived from (1)–(5) as

$$\underline{y}_S = \frac{\underline{i}_{S,\alpha\beta}}{\underline{u}_{S,\alpha\beta}} = \frac{1}{2\jmath\omega_S}\left(\frac{1}{l_d} + \frac{1}{l_q}\right) - \frac{1}{2\jmath\omega_S}\left(\frac{1}{l_d} - \frac{1}{l_q}\right)\frac{\underline{u}^*_{S,\alpha\beta}}{\underline{u}_{S,\alpha\beta}} e^{2\jmath\gamma}. \tag{6}$$

According to the two-axes approximation and neglecting any saturation, this complex admittance is represented by a circle within the complex plane for any constant stator voltage $\underline{u}_{S,\alpha\beta}$.

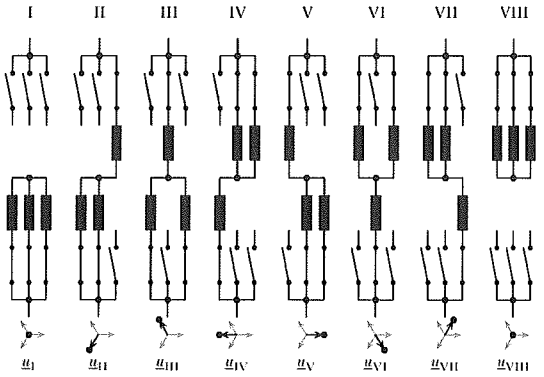

Fig. 1. Possible voltage space phasors of the VSI.

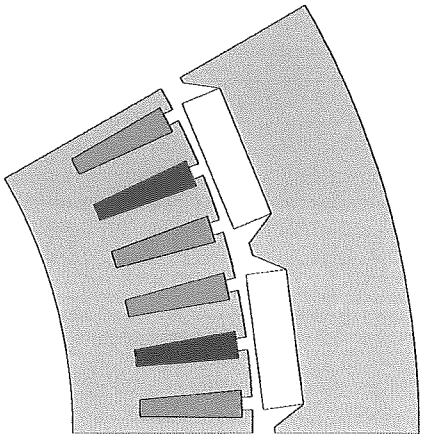

Fig. 2. Cross section of the modeled PMSM with an external rotor, angular rotor position 0°.

These prior considerations suggest the definition of a so-called complex inform reluctance

$$\underline{y}_{\mathrm{INF}} = \underline{y}_0 + \underline{y}_\Delta e^{2\jmath(\gamma-\gamma_u)}. \tag{7}$$

With a constant voltage space vector $\underline{u}_{S,\alpha\beta}$ and the complex inform reluctance (7), the current space vector derivation can be calculated with

$$\dot{\underline{i}}_{S,\alpha\beta} = \underline{y}_{\mathrm{INF}}\underline{u}_{S,\alpha\beta}. \tag{8}$$

According to various applied voltage space vectors $\underline{u}_{S,\alpha\beta}$, the current space vector derivation $\dot{\underline{i}}_{S,\alpha\beta}$ is different in dependence on the angular rotor position, which can be used to obtain the angular rotor position directly from measurements of the current response.

B. Sensorless Drive Concept

According to Fig. 1, a three-phase VSI has eight possible voltage space vectors. There are more or less variations of test pulse patterns that are proposed in former publications [7]. In order to introduce a silent sensorless drive concept, only test pulse patterns that are similar to the regular pulse width modulation (PWM) patterns of the VSI are used.

These test pulse patterns for the sensorless drive concept handle with three voltage space vectors as

$$\underline{u}_{S,\alpha\beta,\mathrm{V}} = \frac{2}{3}u_{\mathrm{DC}} \tag{9a}$$

$$\underline{u}_{S,\alpha\beta,\mathrm{III}} = \frac{2}{3}u_{\mathrm{DC}}e^{\jmath 2\pi/3} \tag{9b}$$

$$\underline{u}_{S,\alpha\beta,\mathrm{II}} = \frac{2}{3}u_{\mathrm{DC}}e^{\jmath 4\pi/3}. \tag{9c}$$

According to these three voltages, there are three measurable finite derivations of the current space vector as

$$\dot{\underline{i}}_{S,\alpha\beta,\mathrm{V}} \approx \frac{\Delta i_{\mathrm{V}}}{\Delta\tau} \tag{10a}$$

$$\dot{\underline{i}}_{S,\alpha\beta,\mathrm{III}} \approx \frac{\Delta i_{\mathrm{III}}}{\Delta\tau}e^{\jmath 2\pi/3} \tag{10b}$$

$$\dot{\underline{i}}_{S,\alpha\beta,\mathrm{II}} \approx \frac{\Delta i_{\mathrm{II}}}{\Delta\tau}e^{\jmath 4\pi/3}. \tag{10c}$$

These current derivations define three complex values of the complex inform reluctance (7). In order to eliminate the reluctance offset $\underline{y}_0$, these three values are combined as given by

$$\begin{aligned}\underline{y}_\Delta e^{2\jmath\gamma} &= \frac{\underline{y}_{\mathrm{INF,V}} + e^{\jmath 4\pi/3}\underline{y}_{\mathrm{INF,III}} + e^{\jmath 8\pi/3}\underline{y}_{\mathrm{INF,II}}}{3} \\ &= \frac{1}{2u_{\mathrm{DC}}\Delta\tau}\left(\Delta i_{\mathrm{V}} - \frac{1}{2}\left(\Delta i_{\mathrm{III}} + \Delta i_{\mathrm{II}}\right)\right. \\ &\qquad \left. + \jmath\frac{\sqrt{3}}{2}\left(\Delta i_{\mathrm{III}} - \Delta i_{\mathrm{II}}\right)\right).\end{aligned} \tag{11}$$

Consequently, the measured current derivations (10) allow for an evaluation of the angular rotor position.

III. Finite Element Modeling

Fig. 2 depicts the 2-D finite element model of the concerned PMSM with an external rotor. To reflect the periodicity of the magnetic field, this two pole model has repeating periodic boundary conditions at the boundaries being two pitches apart. As shown, the stator winding is a full pitch winding and the permanent magnets in the rotor are surface mounted.

Fig. 3 depicts the direct coupling of the 2-D finite element model and the external circuit representing resistances and leakage inductances of the Y-connected stator winding as well as the impedances necessary for the direct application of the phase voltages. With the resistances R_{10}, R_{20}, R_{30} and the applied currents i_{10}, i_{20}, i_{30}, the time-dependent voltages of the VSI u_{10}, u_{20}, u_{30} are applied to the finite element model. In order to fully include the effects of the Y-connected stator winding, the common potential of the three windings can float without any further assumption.

Fig. 4 depicts the time-dependent voltages applied to the external circuit as shown in Fig. 3 representing the test signal injection of the VSI. In order to avoid an offset in the computed phase currents, these applied voltages are modified in such a way that the time-averaged mean value follows to zero.

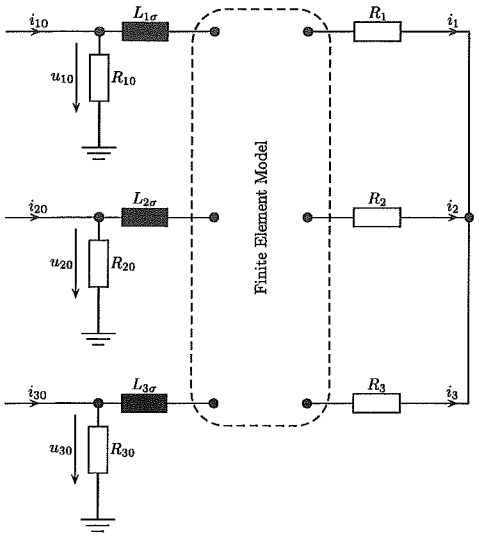

Fig. 3. Direct coupling of external circuit and finite element model.

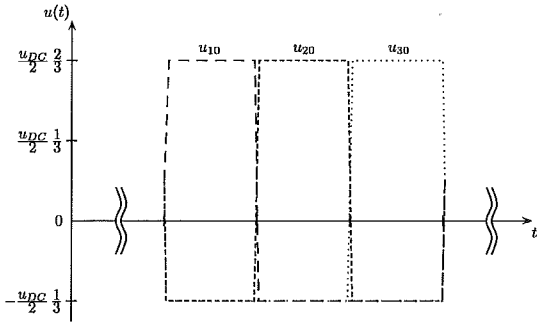

Fig. 4. Time-dependent voltage excitation, total time interval of 3 × 83.333 μs = 250 μs.

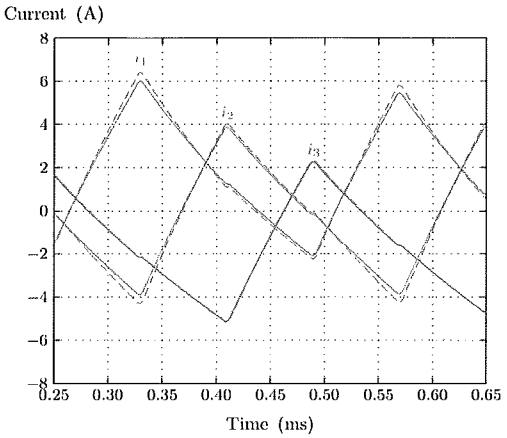

Fig. 5. Numerical current response of all phases, angular rotor position 0°, skewed stator slots (solid lines) and unskewed stator slots (dashed lines).

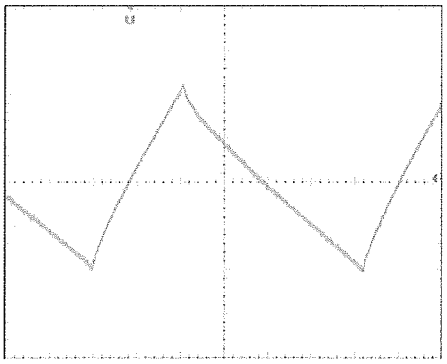

Fig. 6. Measured current response of the phase 2, angular rotor position 0°, time interval 40 μs, current interval 2 A.

A. Sliding Surface and Multislice Approach

In order to create a very fast environment for the analysis of subsequent angular rotor positions, the complete finite element model is constructed from distinct stator and rotor parts, which are coupled together by using a concentric sliding surface within the air gap.

With the sliding surface method, two interface approaches are commonly used, the locked-step modeling and the interpolation modeling [1], [2], [8]. With both approaches, a remeshing of the air-gap regions is avoided yielding an identical quality of the numerical results for all analyses of subsequent angular rotor positions [4], [9], [10]. With the applied locked-step modeling, the possible angular rotor positions are determined by the equidistant discretization of the sliding surface in moving direction.

Second, a multislice approach takes into account the skewing of the stator slots. With this approach, several cross sections along the machine shaft with different angular rotor positions according to the skewing are solved simultaneously within one analysis [3], [11], [12]. As proposed in [12], a Gauss discretization with five cross sections along the axial length of the machine is implemented to achieve a small skew discretization error.

In our case of voltage-driven analyses with unknown currents in both the stator windings and the surface mounted permanent magnets, special attention has to be paid to the coupling of the various slices. This coupling is done with multipoint constraints by assuming a uniform current flow across the different slices. In case of the stator windings, the unknown stator currents of the three windings are constrained to the same but unknown value with each of the various slices. The inclusion of the eddy current flow within the permanent magnets is a more difficult task. Within each of the modeled slices, the distribution of the eddy currents can be different, but the total eddy current flow has to be constrained to the same but unknown value with each of the permanent magnets separately. This can be done by introducing multipoint constraints across each of the permanent magnets in the various slices. Nevertheless, the advantage of significantly less calculation times in comparison to an alternative 3-D finite element model is preserved.

IV. Analysis Results and Measurements

Fig. 5 shows the response of all phase currents i_1, i_2, i_3 according to the applied time-dependent voltages of Fig. 4 for both unskewed and skewed stator slots for the angular rotor position of $\gamma = 0°$. Due to the skewing, the current response slightly

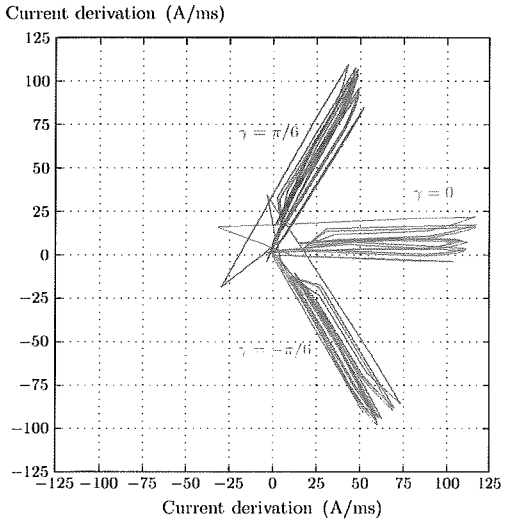

Fig. 7. Numerical current derivation for various angular rotor positions, skewed stator slots.

TABLE I
COMPARISON BETWEEN ANGULAR ROTOR POSITION AND NUMERICALLY ROTOR POSITION, SKEWED STATOR SLOTS

Angular rotor position	Mean value	Standard deviation
0.00	2.23	1.65
-30.00	-27.37	0.90
30.00	30.47	2.28

changes representing lower current derivations with the skewed arrangement in comparison to the unskewed arrangement.

In order to compare the numerical simulations with measurements, Fig. 6 shows the current response according to the applied voltages obtained from measurements. Obviously, there is a good agreement between measured and simulated current response as shown in Fig. 5.

Fig. 7 shows the current derivations according to (11) obtained from the numerical results of the stator current space vector $\underline{i}_{S,\alpha\beta}$ for the angular rotor positions of $\gamma = -30°$, $\gamma = 30°$ and $\gamma = 0°$. Table I lists mean value and standard deviation of these distributions. Consequently, the actual rotor position γ can be evaluated from the algorithm (11) quite accurately.

V. CONCLUSION

This paper discusses voltage-driven finite element analyses of a PMSM with skewed stator slots and an external rotor according to high-frequency voltage pulses. The strong circuit coupling applied with the finite element model allows for a direct excitation with time-dependent voltages of a VSI according to a sensorless drive concept. The indent of these high-frequency voltage pulses lies in the evaluation of position-dependent inductances of the PMSM. The numerically obtained phase currents according to the VSI voltage pulses and the calculated inductances are successfully compared to the results obtained from measurements. Consequently, voltage-driven finite element analyses with a strong circuit coupling can predict the transient behavior of the PMSM in an appropriate way in order to design the machine with an optimum capability for an application in a sensorless electrical drive.

REFERENCES

[1] T. W. Preston, A. B. J. Reece, and P. S. Sangha, "Induction motor analysis by time-stepping techniques," *IEEE Trans. Magn.*, vol. 24, no. 1, pp. 471–474, Jan. 1988.

[2] F. Piriou and A. Razek, "A model for coupled magnetic-electric circuits in electric machines with skewed slots," *IEEE Trans. Magn.*, vol. 26, no. 2, pp. 1096–1100, Mar. 1990.

[3] S. L. Ho and W. N. Fu, "A comprehensive approach to the solution of direct-coupled multislice model of skewed rotor induction motors using time-stepping eddy-current finite element method," *IEEE Trans. Magn.*, vol. 33, no. 3, pp. 2265–2273, May 1997.

[4] E. Schmidt, "Electromagnetic finite element analysis of electrical machines using domain decomposition and floating potentials," in *Proc. 13th Conf. Comput. Electromagn. Fields*, Evian, France, 2001, pp. 38–41.

[5] H. De Gersem, R. Mertens, D. Lahaye, S. Vandewalle, and K. Hameyer, "Solution strategies for transient, field-circuit coupled systems," *IEEE Trans. Magn.*, vol. 36, no. 4, pp. 1531–1534, Jul. 2000.

[6] P. K. Kovacs, *Transient Phenomena in Electrical Machines*. Amsterdam, The Netherlands: Elsevier, 1984.

[7] U.-H. Rieder, "Optimierung Der Sensorlosen Regelung von Permanentmagneterregten Aussenläufer-Synchronmaschinen.," (in German) Ph.D. dissertation, Vienna Univ. Technol., Vienna, Austria, 2005.

[8] I. Tsukerman, "Accurate computation of ripple solutions on moving finite element meshes," *IEEE Trans. Magn.*, vol. 31, no. 3, pp. 1472–1475, May 1995.

[9] H. De Gersem and T. Weiland, "Harmonic weighting functions at the sliding surface interface of a finite element machine model incorporating angular displacement," *IEEE Trans. Magn.*, vol. 40, no. 2, pp. 545–548, Mar. 2004.

[10] M. Ion, H. De Gersem, M. Wilke, and T. Weiland, "Sliding surface interface conditions for 3D machine models discretized by the finite integration technique," *Int. J. Comput. Math. Electr. Electron. Eng.*, vol. 25, no. 2, pp. 427–439, 2006.

[11] D. Rodger, H. C. Lai, and P. J. Leonard, "Coupled elements for problems involving movement," *IEEE Trans. Magn.*, vol. 26, no. 2, pp. 548–550, Mar. 1990.

[12] J. Gyselinck, L. Vandevelde, and J. Melkebeek, "Multi-slice finite element modeling of electrical machines with skewed slots—The skew discretization error," *IEEE Trans. Magn.*, vol. 37, no. 5, pp. 3233–3237, Sep. 2001.